Atmospheric Aerosols in the surrounding area of Lisbon: composition, sources and trends

F. Garcia[1], S.M. Almeida[1] e C.A. Alves[2]

[1] Centro de Ciências e Tecnologias Nucleares, Instituto Superior Técnico, Universidade de Lisboa, Estrada Nacional 10, 2695-066 Bobadela-LRS, Portugal.

[2] Department of Environment and Planning, University of Aveiro, Aveiro, 3810-193, Portugal

Presenting author email: *filipa.pinto.garcia@ist.utl.pt*

Abstract

Throughout 2020, particulate material was collected from Bairro de S. Francisco, in Camarate, a residential area in the north boundary of Lisbon that, due to its geographical location, presents very peculiar characteristics regarding its atmospheric composition. This study aims to estimate the contribution of anthropogenic sources to the atmospheric aerosol, as well as to assess the impact of COVID-19 on particulate matter concentration levels. PM_{10} sampling was performed by a Leckel MVS6 sampler, between February and September 2020, and its chemical composition was determined by PIXE technique (Na, Mg, Al, Si, P, S, Cl, K, Ca, Ti, V, Cr, Mn, Fe, Ni, Cu, Zn, As, Br, Sr, and Ba), ionic chromatography (Na^+, NH_4^+, K^+, Mg^{2+}, Ca^{2+}, Cl^-, NO_3^- and SO_4^{2-}) and through a method of analysis of multiple wavelengths (black carbon (BC)). The results showed that NO_3^- and BC represent the major components of the aerosol, contributing, on average, to about 17% of the PM_{10} mass. It was also noted the presence of some trace elements, such as Zn, Mn, P, Cu, Ba, Cr, V, As and Ni, related to the emissions from fossil fuels combustion, non-exhaust emissions from road traffic and the transformation of industrial materials. In the post-lockdown sampling period, a 39% reduction of the average PM_{10} concentration was observed, with As, Cu, K, Zn, K^+ and NO_3^- having their concentrations reduced over 50%.

Keywords: Atmospheric Aerosol; PM_{10}; Lisbon; Anthropogenic Emissions; Road Traffic; COVID-19

1. Introduction

There is no doubt air is an essential element of life, which is why air quality is a fundamental parameter when approaching environmental health and good quality of life for a population.

There are many sources of air pollution, these differ from region to region and are dependent on several factors, such as level of urbanization, traffic density and the types of industries present in the region, being the highest levels of atmospheric pollution usually associated with urban or industrial areas.

The north region of Lisbon presents a special interest in this matter due to its peculiar characteristics, related to its geographical position. By being located in an industrial/urban area, heavily industrialized and with high population density, contributing to the increase in the intensity of traffic, it has an atmospheric composition with very particular characteristics.

Several studies have shown that particulate matter is among the most harmful pollutants to human health, being strongly linked with the increase of respiratory and cardiovascular diseases (Dockery & Pope III, 1994; Eljarrat et al., 2020; Heal et al., 2012; Schwartz et al., 1996). According to data from the European Environment Agency (EEA), in 2018 the exposure to fine particulate matter ($PM_{2.5}$), in Europe, was responsible for approximately 417.000 premature deaths (EEA, 2020a).

The morphological, chemical, physical, and thermodynamic properties of particulate matter in the atmosphere vary with space and time, being affected by local and regional events, such as the influence of sources with distinct characteristics and the chemical transformations that can occur in the atmosphere, as well as continentally or globally, which involve long-range transport over long periods of times (Almeida, 2004).

The characterization of atmospheric particulate matter focuses on several parameters, such as number, concentration, density, mass, size, chemical composition and optical properties (Seinfeld & Pandis, 1998). The risk associated with inhaling particulate matter depends on their characteristics, such as size, shape, density, and reactivity, as well as where they settle in the respiratory system (Heyder, 2004; Schwartz et al., 1996). Depending on their chemical composition, the accumulation of particulate matter can also lead to negative impacts in the environment, due to their influence on the energy balance on the surface of the Earth, reducing visibility, forming clouds, and affecting heat exchanges in the atmosphere, contributing to climate change (EEA, 2021).

The emission of the main air pollutants, in Europe, has been decreasing since 1990, according to data from the EEA, between 2000 and 2018, the emission of PM_{10} suffered a reduction of 29%, with the industrial sector reaching the highest decrease (EEA, 2020b). In the spring of 2020, the lockdown measures implemented in most European countries, to reduce the spread of COVID-19, lead to a sudden reduction of economic activities, including a drop in the transportation sector, leading to a decrease in atmospheric pollutants emissions and therefore a reduction in their concentrations. Data from EEA member-states illustrate how the concentration of NO_2 and PM_{10} decreased in several cities during the lockdown period, with the mean reduction observed on pollutant concentrations being higher for NO_2 (60%) than for PM_{10} (30%) and being more significant in traffic areas (EEA, 2020a). The impact analysis of the applied measures in the reduction of these pollutants allows us to understand more clearly what happened regarding atmospheric pollution, being undeniable that the reduction in the concentrations of NO_2 and PM_{10} appear as a result of COVID-19 lockdown measures, due to a severe reduction in human activity in sectors such as transports and industrial activities (EEA, 2020a; Rodrigues & Monteiro, 2020).

Even though measures to reduce exposure to atmospheric pollutants have been increasing all over the world, the degradation of air quality is still a problem. The study of atmospheric particulate matter allows for the identification of their main sources as well as to evaluate their contribution to air pollution, making it possible to develop means to control emissions and more localized prevention measures. Hence, this report focuses on providing a general overview of the contribution of the main sources of pollutants to the concentration of PM_{10}, in the north edge of Lisbon, and evaluating the impact of COVID-19 lockdown restrictions on air quality.

2. Materials and methods

2.1. Site description

Sampling was performed in a primary school, in Bairro de S. Francisco, in Camarate, a sub-urban and industrial area, on the outskirts of Lisbon. The sampling station (*Fig. 1*) was located 450m from Lisbon Airport and thus surrounded by a great variety of industrial activities, including a bituminous concrete factory production unit (350m) and several high density traffic roads (1 km from CRIL/A36/IC17, 700m from Eixo Norte-Sul/IP7 and 600m from Av. Santos e Castro, which connects Segunda-Circular to Eixo Norte-Sul), influenced by the commuting movements of people on their way to and from work between the city and residential areas in the north of Lisbon. The parish of Camarate is in the south municipality of Loures, on the right side of the Tagus Estuary valley, approximately 2.5 km from the Trancão river and about 20km from the Atlantic Ocean.

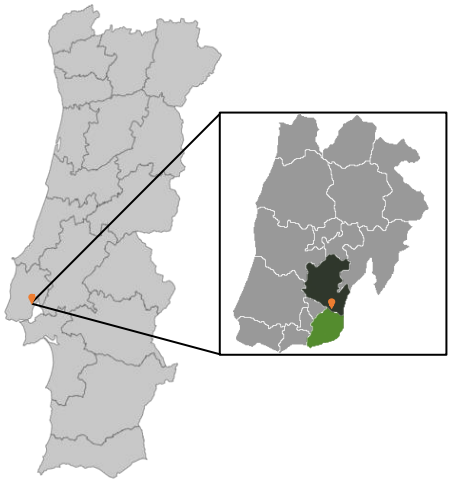

Fig. 1 - Sampling site localization ( ) in Portugal and in Lisbon Metropolitan Area (Light green pattern – Lisbon; Dark green pattern – Loures).

2.2. Description of the sampling equipment

A Leckel MVS6 sampler was used to collect PM_{10} on 47 mm Teflon filters, with 2 µm pore size and a Polypropylene support ring at a flow rate of 2.3 m^3/h.

A total of 40 PM samples were collected between March and September of 2020. The sampling was done over 24 h periods, typically five times a week, with one sample collected on a Sunday.

2.3. Gravimetric and chemical analysis

The filter loads were determined by gravimetry using a 0.1 µg sensitivity balance (Mettler Toledo, UMT5) in a controlled cleanroom. The mass of the filter before and after sampling was obtained as the average of three measurements.

For the chemical characterization, filters were analyzed by Particle Induced X-Ray Emission (PIXE) for the measurement of major and trace elements (Na, Mg, Al, Si, P, S, Cl, K, Ca, Ti, V, Cr, Mn, Fe, Ni, Cu, Zn, As, Br, Sr, and Ba), by Ion Chromatography for the measurement of water-soluble ions (Na^+, NH_4^+, K^+, Mg^{2+}, Ca^{2+}, Cl^-, NO_3^- e SO_4^{2-}), and with the Multi-wavelength absorption black carbon instrument (MABI) for Black Carbon (BC).

2.4. Air mass back trajectories

To identify the possible sources of dust, which impacts sampling, four days backward trajectories, ending in Camarate, were calculated using the HYSPLIT model (Rolph et al., 2017; Stein et al., 2015) at 50, 500, and 1000 m height and the vertical velocity option.

2.5. Mass closure

PM_{10} results were subjected to a Mass Closure (MC) test to determine whether the measurement of gravimetric PM concentration of a sample is equal to the sum of the concentrations of the individually identified species. This test was used to check data consistency, to characterize the relative contribution of the different components to PM.

MC was calculated including the assessment of the contribution of mineral aerosol, marine aerosol, anthropogenic species, BC, non-marine sulfate ($SO_4^{2-}{}_{nm}$), NO_3^- and NH_4^+. In MC some approximations were made to infer some unmeasured chemical species. The sum of the chemical species in the aerosol with values lower than the total mass concentration indicates the existence of an unidentified mass (UM). The contribution of each aerosol type source was calculated according to the equations presented in *Table 1*.

The mineral aerosol was determined considering the oxides of Al, Si, Ca, K, Fe, Ti, Mn and Ba, and the soil fractions of Ca, K and Fe, calculated using their typical crustal ratios (Mason & Moore, 1982). The marine aerosol was calculated through the sum of Na^+, Cl^-, Mg^{2+} and the marine fractions of $K^+{}_m$, $Ca^{2+}{}_m$ and $SO_4^{2-}{}_{m,}$ also Br and Sr were added to this fraction (Bowen, 1979). The elements V, Cr, Ni, Cu, Zn, As and P and the anthropogenic fractions of K, Ca and Fe were associated with the anthropogenic aerosol type sources group. BC, $SO_4^{2-}{}_{nm}$, NO_3^- and NH_4^+ were considered separately from any group.

Table 1 - Equations used to calculate the source contribution based on Mass Closure.

Sources	Equations	
Mineral aerosol	$1.89[Al] + 2.14[Si] + 1.67[Ti] + 1.4[Ca_{soil}] + 1.2[K_{soil}] + 1.4[Fe_{soil}] + 1.58[Mn] + 1.12[Ba]$	$[Ca_{soil}] = 0.45 \times [Al]$ $[K_{soil}] = 0.32 \times [Al]$ $[Fe_{soil}] = 0.62 \times [Al]$
Marine aerosol	$[Na^+] + [Cl^-] + [Mg^{2+}] + [Br] + [Sr] + [K^+_m] + [Ca^{2+}_m] + [SO_4^{2-}_m]$	$[K^+_m] = 0.037 \times [Na^+]$ $[Ca^{2+}_m] = 0.038 \times [Na^+]$ $[SO_4^{2-}_m] = 0.25 \times [Na^+]$
Anthropogenic species	$[K_{anthropogenic}] + [Ca_{anthropogenic}] + [Fe_{anthropogenic}] + [V] + [Cr] + [Ni] + [Cu] + [Zn] + [As] + [P]$	$[K_{anthropogenic}] = [K] - [K_{soil}] - [K^+_m]$ $[Ca_{anthropogenic}] = [Ca] - [Ca_{soil}] - [Ca^{2+}_m]$ $[Fe_{anthropogenic}] = [Fe] - [Fe_{soil}]$
$SO_4^{2-}{}_{nm}$	$[SO_4^{2-}] - [SO_4^{2-}_m]$	

2.6. Statistical analysis

Statistical analysis of all data was performed using the STATISTICA® software. An analysis of variance of the results was performed using nonparametric statistics at a significance level of $p<0.05$. The Mann–Whitney U test was used to compare differences between independent samples (for the variables Pre-Lockdown/Post-Lockdown). Correlations between components were expressed by Spearman (ρ) correlation coefficients, to better comprehend the origin of the particles and their constitution.

3. Results and discussion

The average mass concentrations of PM_{10} and major chemical components are summarized in *Table 2*. The PM_{10} mass concentration at Bairro de S. Francisco varied between 5.1 and 48 µg/m^3 and had a mean value of 25.9 µg/m^3. PM_{10} average concentration is below the EU annual PM_{10} limit value of 40 µg/m^3 even though it stayed above the WHO guidelines for annual PM_{10} (20 µg/m^3). The EU 24h PM_{10} limit value of 50 µg/m^3 was not exceeded by any sample.

The most abundant species in PM_{10} were BC, Cl^-, NO_3^-, Na^+, SO_4^{2-} and Ca^{2+}. The industrial/urban characteristics of the study site cause species with an anthropogenic origin, such as BC, SO_4^{2-} and NO_3^-, to represent major components in the aerosol. However, the concentration of these components are lower than those in other European urban areas (Bressi et al., 2021). This is likely due to Portugal's location relative to the ocean, which promotes a higher dispersion of pollutants.

Portuguese coastal areas have an important input of marine aerosol, which translates to high concentrations of sea salt species, Cl^- and Na^+ in the atmospheric aerosol. Al, Si, Fe and Ca are typical soil elements, representing the crustal contribution for the mineral aerosol.

Table 2 - Mean PM_{10} and component concentrations for the study period (in ng/m^3).

	Mean ± SD*		Mean ± SD*
PM_{10}	25942 ± 10451	K	315 ± 205
Na^+	1590 ± 1418	Ca	2049 ± 1488
NH_4^+	316 ± 171	Ti	36 ± 22
K^+	150 ± 124	V	2.3 ± 13
Mg^{2+}	178 ± 134	Cr	6.7 ± 5.6
Ca^{2+}	1097 ± 669	Mn	22 ± 17
Cl^-	1988 ± 1720	Fe	555 ± 295
NO_3^-	1871 ± 1227	Ni	0.88 ± 0.66
SO_4^{2-}	1460 ± 595	Cu	10 ± 8.1
Na	2023 ± 1105	Zn	23 ± 13
Mg	360 ± 169	As	1.7 ± 1.9
Al	454 ± 292	Br	7.1 ± 4.5
Si	1007 ± 606	Sr	2.1 ± 13
P	18 ± 9.8	Ba	6.5 ± 2.7
S	729 ± 288	BC	2627 ± 1322
Cl	2363 ± 1844		

* Standard deviation;

3.1. Source apportionment

3.1.1. Marine aerosol

The Cl^- and Na^+ high concentrations can be easily related with ocean contribution due to the geographic

position of the sampling site. Chloride main source in atmospheric aerosols are emissions from sea salt that are mainly associated with sodium originated in sea spray (Viana et al., 2008), therefore these ions represent the main source of marine aerosols in this area.

Magnesium mainly originates in crustal sources and can also have marine origins, a high positive correlation coefficient between Cl^-, Na^+, and Mg^{2+}, indicates that they have a common source, which could be attributed to the sea salt. The Spearman rank order correlation matrix also indicates a strong correlation between Sr, Br, K^+ and SO_4^{2-} and the marine aerosol. A spearman rank correlation analysis for these components is showed in *Table 3*.

3.1.2. Mineral aerosol

The mineral aerosol has a composition very similar to the soil, rich in Si, Al, Fe, Ca, K, Ti, Mn e Ba (Rudnick & Gao, 2013; Viana et al., 2008; Wedepohl, 1995). The data in *Table 3* confirms that there are medium to strong correlations between these elements revealing the existence of one major common source, which is probably the crust.

The dust released into the air depends on several factors related to the soil and weather conditions. Therefore chemical composition of the dust particles is dependent on the soil and location where they originate from. Mineral dust is generated by the action of wind on the Earth's surface and the main sources are deserts or semi-arid surfaces (Calvo et al., 2013). In South European regions, such as Portugal, the presence of dust particles is particularly noted in mass transport events, originated from the North of Africa (Almeida et al., 2005; Rodríguez et al., 2002). The origin of these elements could be clarified from the projection of the air mass backward trajectories obtained by the NOAA HYSPLIT model, based on the behavior of the air masses in the time interval of 6h before the start of the sampling.

According to the backtracking trajectories, air masses arriving in Camarate during February 6th, 2020 were associated with south Continental air masses from the North of Africa (*Fig. 2).* These trajectories were selected for display since it corresponds to the highest mass concentration of PM_{10} recorded throughout the sampling period (48 $\mu g/m^3$). This is due to an important contribution of long range transported soil emissions. Moreover, the observed concentrations of the predominant elements in the mineral aerosol originated from the North of Africa (Cardoso, 2016), Si (1612 ng/m^3), Al (628 ng/m^3), Mg (526 ng/m^3), Ca (2702 ng/m^3), Fe (964 ng/m^3), Ti (46 ng/m^3), Mn (25 ng/m^3) and Sr (5 ng/m^3), were higher in this sampling, when compared to the average concentrations.

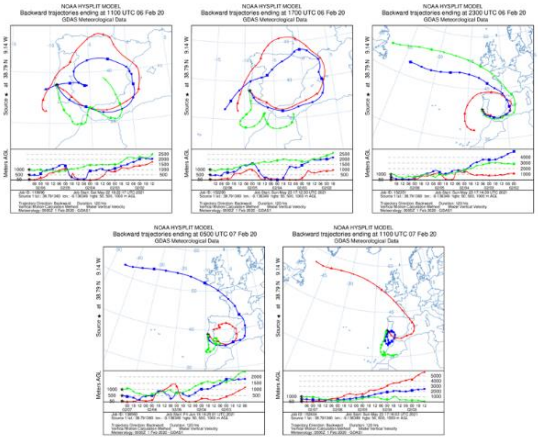

Fig. 2 - HYSPLIT model backward trajectories, arriving at sampling site between 11 h of February 6 and 11 h of February 7. Based on the behavior of the air masses at the time interval of 6 h.

In cities, the non-exhaust emissions from road traffic can be important sources of mineral dust. Elements such as Ca, K and Fe show medium to strong correlations with Zn, P, As, Cu and V, some of them can be associated with mineral aerosols although they mainly come from anthropogenic sources like road traffic mainly due to dust resuspension, erosion of road pavements and tires and brake wear.

3.1.3. Trace elements

The presence of some vestigial elements such as Zn, Mn, P, Cu, Ba, Cr, V, As, and Ni, in the atmospheric aerosol, can be attributed to anthropogenic emissions, mainly by road traffic (from fossil fuels combustion and non-exhaust emissions)

Table 3 - Spearman correlation coefficient between particulate species. (Grey – Strong correlations)

Variables	Al	Si	P	K	Ca	Ti	V	Cr	Mn	Fe	Ni	Cu	Zn	As	Br	Sr	Ba	Na^+	NH_4^+	K^+	Mg^{2+}	Ca^{2+}	Cl^-	NO_3^-	SO_4^{2-}	BC
Al		**0.95**	0.73	0.69	0.66	0.76	0.62	0.46	0.63	0.68	0.42	0.46	0.59	0.56	0.37	0.52	0.51	0.21	0.14	0.53	0.31	0.64	0.10	0.42	0.61	0.41
Si			0.81	0.79	0.79	0.85	0.72	0.56	0.67	0.82	0.53	0.61	0.72	0.67	0.48	0.51	0.63	0.25	0.18	0.63	0.38	0.79	0.17	0.54	0.62	0.55
P				0.88	0.65	0.62	0.48	0.50	0.58	0.87	0.50	0.83	0.80	0.84	0.48	0.33	0.55	0.11	0.27	0.81	0.26	0.66	0.04	0.63	0.31	0.80
K					0.61	0.68	0.61	0.45	0.46	0.81	0.59	0.83	0.82	0.89	0.65	0.48	0.58	0.27	0.43	**0.93**	0.41	0.70	0.19	0.80	0.52	0.83
Ca						0.84	0.65	0.87	0.89	0.88	0.44	0.59	0.75	0.54	0.43	0.40	0.74	0.28	-0.11	0.48	0.46	**0.93**	0.37	0.40	0.35	0.46
Ti							0.76	0.71	0.75	0.79	0.47	0.52	0.72	0.54	0.46	0.42	0.80	0.27	0.15	0.47	0.40	0.80	0.28	0.49	0.60	0.47
V								0.47	0.50	0.59	0.60	0.36	0.54	0.39	0.38	0.33	0.57	0.19	0.32	0.47	0.26	0.67	0.17	0.54	0.64	0.40
Cr									**0.93**	0.78	0.37	0.46	0.68	0.49	0.34	0.26	0.65	0.15	-0.11	0.30	0.35	0.74	0.30	0.27	0.19	0.32
Mn										0.78	0.31	0.44	0.65	0.44	0.27	0.31	0.63	0.15	-0.19	0.31	0.33	0.76	0.25	0.23	0.22	0.32
Fe											0.50	0.82	**0.91**	0.78	0.55	0.38	0.77	0.25	0.14	0.70	0.46	0.85	0.26	0.61	0.35	0.72
Ni												0.43	0.50	0.45	0.52	0.15	0.38	0.15	0.62	0.51	0.12	0.48	0.10	0.73	0.59	0.50
Cu													0.77	0.83	0.46	0.26	0.57	0.11	0.29	0.81	0.27	0.65	0.12	0.63	0.19	0.90
Zn														0.79	0.56	0.33	0.68	0.22	0.24	0.72	0.42	0.77	0.23	0.62	0.35	0.69
As															0.54	0.41	0.54	0.14	0.35	0.84	0.33	0.60	0.09	0.63	0.30	0.81
Br																0.64	0.45	0.77	0.31	0.59	0.78	0.52	0.69	0.74	0.62	0.47
Sr																	0.40	0.78	0.02	0.46	0.76	0.48	0.70	0.37	0.55	0.19
Ba																		0.32	0.21	0.48	0.43	0.71	0.38	0.49	0.41	0.52
Na^+																			0.02	0.26	0.87	0.34	**0.93**	0.38	0.55	0.04
NH_4^+																				0.40	-0.09	-0.04	-0.11	0.66	0.55	0.47
K^+																					0.37	0.61	0.20	0.76	0.38	0.83
Mg^{2+}																						0.53	0.85	0.41	0.45	0.15
Ca^{2+}																							0.43	0.50	0.39	0.55
Cl^-																								0.26	0.41	0.00
NO_3^-																									0.63	0.73
SO_4^{2-}																										0.28
BC																										

and from the transformation of industrial resources (Calvo et al., 2013; Viana et al., 2008), as well as originated from the soil.

Strong correlations between these elements with those associated with mineral dust, allows for the differentiation of their source. The combination of elements associated with mineral dust with Cu, Mn, Ni and Zn, are usually related to mechanical abrasion of tires while Fe, Ba, Zn and Cu are frequently related with brake abrasion (Calvo et al., 2013; Viana et al., 2008). Also, the strong correlations with V and Ni can be associated to the burning fuel oil (Viana et al., 2008), while those with P relate to the burning of biomass and/or fossil fuels and agriculture fertilizers. Correlations between Cr and Mn with elements present in mineral dust suggest a common origin, associated with emission of exhaust gases and particles originated from vehicle's brakes.

As such, Fe can be originated in the wear of vehicle's brakes, contributing, in part, Fe-Ca (ρ=0.88) and Fe-Ti (ρ=0.79) from the dust originated from the resuspension of soil by local road traffic. Potassium also shows a strong correlation pattern with elements from anthropogenic sources, namely As (ρ=0.89), P (ρ=0.88), Cu (ρ=0.83), Zn (ρ=0.82) and BC (ρ=0.83). The correlations between these elements are also strong, which suggest a common source between K, As, P, Cu, Zn and BC that could result from coal combustion and biomass burn.

From the analysis, it is concluded that there is a predominant anthropogenic influence, associated mainly with road traffic and burning of fossil fuels.

3.1.4. Ammonium, sulphate, nitrate, and black carbon

$SO_4^{2-}{}_{nm}$, NH_4^+, NO_3^- and black carbon are major components of the aerosols therefore, they were considered separately.

Between the secondary inorganic ions NO_3^-, NH_4^+ and SO_4^{2-}, the ions SO_4^{2-} and NO_3^- show a moderate correlation with NH_4^+ (ρ=0.55 and ρ=0.66, respectively). This association tendency reflects the existence of NH_4^+ in the samples, in the form of sulphate and nitrate salts ($(NH_4)_2SO_4$ and NH_4NO_3, respectively). In the summer, SO_4^{2-} and NH_4^+ present a higher association, since the stronger solar radiation causes an increase in temperature and contributes to the formation of OH radicals, promoting the formation of secondary sulphates such as $(NH_4)_2SO_4$ (Almeida et al., 2009; Querol et al., 2008). On the other hand, in the winter, NH_4^+ is in

excess, in relation to SO_4^{2-} and is therefore also associated with NO_3^- leading to the formation of NH_4NO_3. In warm seasons, NO_3^- is, in part, attributed to the reaction of HNO_3^- with mineral species such as calcium carbonate and sea salt, forming $Ca(NO_3)_2$ and $NaNO_3$, respectively (Almeida et al., 2005).

Black carbon arises from the burning of carbonaceous fuels in urban areas, predominantly from road traffic. The Spearman correlation coefficients identified strong correlations between BC and NO_3^- (ρ=0.73), Cu (ρ=0.90), K (ρ=0.83), As (ρ=0.81), P (ρ=0.80) and Fe (ρ=0.72) which proves the origin of As, Cu, K, Fe, P e NO_3^- from combustion and incineration processes mainly from road traffic.

3.1.5. Mass Closure

By performing a mass closure, the PM_{10} mass concentrations obtained by gravimetric analysis were compared to the sum of the identified species, to determine the contribution of the different aerosol types and quantify the percentage of non-identified compounds in the analysis. *Fig. 3* presents the contribution of each chemical compound/aerosol type to the PM_{10} mass.

The aerosols were divided into seven chemical compound/aerosol types: mineral aerosol, marine aerosol, anthropogenic species, BC, non-marine sulphate ($SO_4^{2-}{}_{nm}$), NO_3^- and NH_4^+. The study of Spearman correlation coefficients between the components, allowed for the association of particle species with higher correlations.

On average, the total mass of the measured and estimated species by MC explained 63% of the total PM_{10} mass measured by gravimetry. The remaining fraction can be attributed to organic carbon and carbonates which were not measured in this study, even though there is relevance in their share of the mass concentration. There were also made approximations in the soil composition, and so they might not be an exact representation of the study site. The marine aerosol was the dominant contributor to the total mass of PM_{10} (16%) with the mineral dust accounting for 15% followed by BC and by anthropogenic species with a contribution of 10% and 8.2%, respectively. The sum of SO_4^{2-}nm, NO_3^- and NH_4^+ accounted for 13% of the PM_{10} mass.

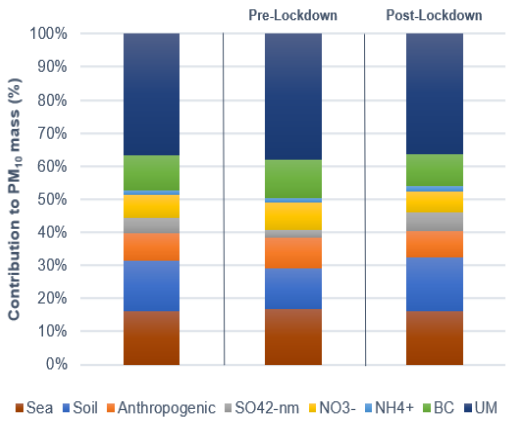

Fig. 3 - Average contribution to PM_{10} of soil, sea, anthropogenic species, BC, $SO_4^{2-}{}_{nm}$, NO_3^- and NH_4^+.

3.1. COVID-19

To understand the impact on air quality, in Bairro de S. Francisco, due to the COVID-19 lockdown, in March 2020, the sampling was divided into two periods: Pre-Lockdown (samples collected between February 2nd and March 12th, 2020), before any Emergency Sate measures were announced in Portugal, and post-lockdown (samples collected between June 17th and September 28th, 2020), after less restrictive lockdown measures have started to be applied.

This study focused on the reduction of the concentrations of PM_{10} chemical compounds, resulting from the lockdown measures, independent from weather patterns, seasonality, and long-distance transport, as well as the traffic flux variation during the weekdays/weekends. A comparison between pre and post-lockdown concentration values was made, and a variation of the extension of their reduction was recorded.

Fig. 4 shows the percentage of the reduction of aerosol components' concentration with a significance level of 0.050 pre and post lockdown. The average concentrations of PM_{10} obtained, show an average reduction of 39%, a considerable impact comparatively to the one recorded at National and European level, where the average reductions were

of about 30% (EEA, 2020a; Gama et al., 2021). As, Cu, K, Zn, and NO_3^- which are usually associated with combustion and incineration processes, as well as road traffic, suffered from extreme decreases reaching more than 50% reduction. In particular, arsenic concentration was the one with a higher decrease of about 69%, with significantly lower concentrations ($p<0.0001$) post-lockdown.

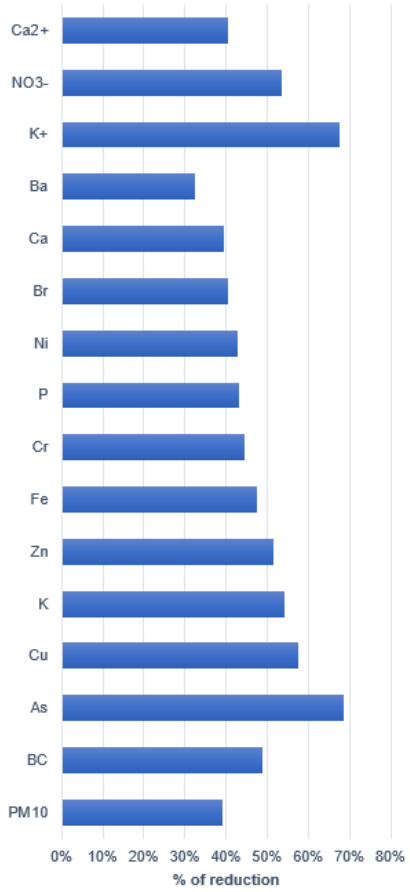

Fig. 4 - Percentage of reduction of aerosol components concentration with statistically significant differences ($p<0.05$) pre and post lockdown.

The MC analysis allows us to evaluate the change in mass contributions of each chemical compound/aerosol types to the total mass of PM_{10} in the pre- and post-lockdown period. *Fig. 3* reveals a decrease in the contribution of the anthropogenic aerosol, together with NO_3^-, $SO_4^{2-}{}_{nm}$, NH_4^+ and BC, to the total mass of PM_{10}, of about 1.7%. This reduction can be justified by the decrease in traffic and trade market, as well as the reduction in labor in several industries, changes that occurred during the lockdown period, as part of the imposed measures to stop the dissemination of COVID-19, leading to a reduction in the emission of atmospheric pollutants.

4. Conclusion

The composition of PM_{10} was investigated to identify the main sources affecting an industrial/urban area with a particular geographical location.

The MC was used to check data consistency and to characterize the relative contribution of different components of PM_{10}. The chemical composition of PM_{10} varies throughout the analysis due to seasonal variations, as well as flux variation during the weekdays/weekends but mainly as a result of the restrictions imposed to stop the dissemination of COVID-19.

The marine and mineral aerosols are major components of PM_{10}, contributing, on average, to about 16 and 15% of the PM_{10} mass, respectively.

Source proportion results show that road traffic and burning of fossil fuels are the main sources of pollutants emissions at the study site. This activity is associated mainly with the emission of NO_3^- and BC, those are major components of the aerosol, contributing, on average, to about 17% of the PM_{10} mass. Zn, Mn, P, Cu, Ba, Cr, V, As, and Ni are also associated with road traffic, due to burning of fossil fuels as well as non-exhaust road traffic emissions (brake and tire wear, pavement abrasion and particle resuspension processes), their contribution to PM_{10} represents about 8.2%.

After identifying the contribution of the PM_{10} sources, it is possible to conclude that there is a predominantly anthropogenic influence in this concentration, mainly associated with traffic and the burning of fossil fuels.

The COVID-19 pandemic had health and economic impacts at a global level, which led to an indirect impact in atmospheric pollution. The decrease of air and road traffic as well as the reduction of labor in several industries, due to the restrictions imposed to stop the dissemination of COVID-19, had a huge impact in the reduction of the concentration of atmospheric pollutants like PM_{10}. This allowed us to have a clearer interpretation of the

impacts of human activity on air pollution and conclude that the abatement strategies to reduce PM emissions and improve air quality, should focus mainly on road traffic and industrial activities.

5. References

Almeida, S. M. (2004). *Composição e origem do aerossol atmosférico em zona urbano-industrial*. Universidade de Aveiro.

Almeida, S. M., Freitas, M. C., Repolho, C., Dionísio, I., Dung, H. M., Pio, C. A., Alves, C., Caseiro, A., & Pacheco, A. M. G. (2009). Evaluating children exposure to air pollutants for an epidemiological study. *Journal of Radioanalytical and Nuclear Chemistry*, *280*(2), 405–409. https://doi.org/10.1007/s10967-009-0535-3

Almeida, S. M., Pio, C. A., Freitas, M. C., Reis, M. A., & Trancoso, M. A. (2005). Source apportionment of fine and coarse particulate matter in a sub-urban area at the Western European Coast. *Atmospheric Environment*, *39*(17), 3127–3138. https://doi.org/10.1016/j.atmosenv.2005.01.048

Bowen, H. J. M. (1979). *Environmental chemistry of the elements*. Academic Press.

Bressi, M., Cavalli, F., Putaud, J. P., Fröhlich, R., Petit, J. E., Aas, W., Äijälä, M., Alastuey, A., Allan, J. D., Aurela, M., Berico, M., Bougiatioti, A., Bukowiecki, N., Canonaco, F., Crenn, V., Dusanter, S., Ehn, M., Elsasser, M., Flentje, H., … Prevot, A. S. H. (2021). A European aerosol phenomenology - 7: High-time resolution chemical characteristics of submicron particulate matter across Europe. *Atmospheric Environment: X*, *10*, 100108. https://doi.org/10.1016/J.AEAOA.2021.100108

Calvo, A. I., Alves, C., Castro, A., Pont, V., Vicente, A. M., & Fraile, R. (2013). Research on aerosol sources and chemical composition: Past, current and emerging issues. *Atmospheric Research*, *120–121*, 1–28. https://doi.org/10.1016/J.ATMOSRES.2012.09.021

Cardoso, J. (2016). *Estudo do Aerossol (poeira do Sara) na região de Cabo Verde.*

Dockery, D. W., & Pope III, C. A. (1994). Acute respiratory effects of particulate air pollution. In *Annu. Rev. Public Health* (Vol. 15).

Dockery, D. W., Pope III, C. A., Xu, X., Spengler, J. D., Ware, J. H., Fay, M. E., Ferris, B. G., Jr., & Speizer, F. E. (1993). An association between air pollution and mortality in six U.S. cities. *The New England Journal of Medicine*, *329*(24), 1753–1759. https://doi.org/10.1056/NEJM199312093292401

EEA. (2020a). Air quality in Europe — 2020 report, EEA Report No 09/2020, European Environment Agency. In *EEA Report*. https://www.eea.europa.eu//publications/air-quality-in-europe-2020-report

EEA. (2020b). *European Union emission inventory report 1990-2018* (Issue 05).

EEA. (2021). *Saúde e ambiente, incluindo poluição atmosférica e sonora — Salientando o trabalho da AEA*. https://www.eea.europa.eu/pt/articles/saude-e-ambiente-incluindo-poluicao

Eljarrat, E., Li, F., Jahangir Alam, M., Stavropoulou, E., Manisalidis, I., Stavropoulos, A., & Bezirtzoglou, E. (2020). Environmental and Health Impacts of Air Pollution: A Review. *Frontiers in Public Health | Www.Frontiersin.Org*, *8*, 14. https://doi.org/10.3389/fpubh.2020.00014

Gama, C., Relvas, H., Lopes, M., & Monteiro, A. (2021). The impact of COVID-19 on air quality levels in Portugal: A way to assess traffic contribution. *Environmental Research*, *193*, 110515. https://doi.org/10.1016/j.envres.2020.110515

Heal, M. R., Kumar, P., & Harrison, R. M. (2012). Particles, air quality, policy and health.

Chemical Society Reviews, *41*(19), 6606–6630. https://doi.org/10.1039/c2cs35076a

Mason, B., & Moore, C. B. (1982). *Principles of Geochemistry*. Wiley, New York.

Pope, C. A., Burnett, R. T., Thun, M. J., Calle, E. E., Krewski, D., Ito, K., & Thurston, G. D. (2002). Lung cancer, cardiopulmonary mortality, and long-term exposure to fine particulate air pollution. *Journal of the American Medical Association*, *287*(9), 1132–1141. https://doi.org/10.1001/jama.287.9.1132

Querol, X., Alastuey, A., Moreno, T., Viana, M. M., Castillo, S., Pey, J., Rodríguez, S., Artiñano, B., Salvador, P., Sánchez, M., Garcia Dos Santos, S., Herce Garraleta, M. D., Fernandez-Patier, R., Moreno-Grau, S., Negral, L., Minguillón, M. C., Monfort, E., Sanz, M. J., Palomo-Marín, R., … Sánchez de la Campa, A. (2008). Spatial and temporal variations in airborne particulate matter (PM10 and PM2.5) across Spain 1999-2005. *Atmospheric Environment*, *42*(17), 3964–3979. https://doi.org/10.1016/j.atmosenv.2006.10.071

Rodrigues, V., & Monteiro, A. (2020). *COVID-19 e a melhoria da qualidade do ar*. Universidade de Aveiro. https://www.ua.pt/pt/noticias/13/62898

Rodríguez, S., Querol, X., Alastuey, A., & Plana, F. (2002). Sources and processes affecting levels and composition of atmospheric aerosol in the western Mediterranean. *J. Geophys. Res*, *107*(D24), 4777. https://doi.org/10.1029/2001JD001488

Rolph, G., Stein, A., & Stunder, B. (2017). Real-time Environmental Applications and Display sYstem: READY. *Environmental Modelling and Software*, *95*, 210–228. https://doi.org/10.1016/j.envsoft.2017.06.025

Rudnick, R. L., & Gao, S. (2013). Composition of the Continental Crust. In *Treatise on Geochemistry: Second Edition* (Vol. 4, pp. 1–51). Elsevier Inc. https://doi.org/10.1016/B978-0-08-095975-7.00301-6

Schwartz, J., Dockery, D. W., & Neas, L. M. (1996). Is Daily Mortality Associated Specifically with Fine Particles? *Journal of the Air and Waste Management Association*, *46*(10), 927–939. https://doi.org/10.1080/10473289.1996.10467528

Seinfeld, J. H., & Pandis, S. N. (1998). Atmospheric chemistry and physics - From air pollution to climate change. In *John Wiley & Sons, Inc.* Springer Berlin Heidelberg. http://link.springer.com/10.1007/978-3-662-04540-4_16

Stein, A. F., Draxler, R. R., Rolph, G. D., Stunder, B. J. B., Cohen, M. D., & Ngan, F. (2015). Noaa's hysplit atmospheric transport and dispersion modeling system. In *Bulletin of the American Meteorological Society* (Vol. 96, Issue 12, pp. 2059–2077). American Meteorological Society. https://doi.org/10.1175/BAMS-D-14-00110.1

Torres, P., Ferreira, J., Monteiro, A., Costa, S., Pereira, M. C., Madureira, J., Mendes, A., & Teixeira, J. P. (2018). Air pollution: A public health approach for Portugal. *Science of the Total Environment*, *643*, 1041–1053. https://doi.org/10.1016/j.scitotenv.2018.06.281

Viana, M., Kuhlbusch, T. A. J., Querol, X., Alastuey, A., Harrison, R. M., Hopke, P. K., Winiwarter, W., Vallius, M., Szidat, S., Prévôt, A. S. H., Hueglin, C., Bloemen, H., Wåhlin, P., Vecchi, R., Miranda, A. I., Kasper-Giebl, A., Maenhaut, W., & Hitzenberger, R. (2008). Source apportionment of particulate matter in Europe: A review of methods and results. *Journal of Aerosol Science*, *39*(10), 827–849. https://doi.org/10.1016/j.jaerosci.2008.05.007

Wedepohl, K. H. (1995). The composition of the continental crust. *Geochimica et Cosmochimica Acta*, *59*(7), 1217–1232. https://doi.org/10.1016/0016-7037(95)00038-2